

## Flow Under A Depressed Weir on Anisotropic Porous Medium of Infinite Depth

by

A. S. Reddy\*

U. Basu\*\*

### Introduction

Seepage characteristics have been already studied for the case of flow under a depressed weir embedded in an isotropic medium (Pavlovsky; vide Harr, 1962). Analytical solutions were given separately by Pavlovsky for the cases when the underlying permeable stratum is of infinite depth, and also when the stratum extends to a finite depth.

The purpose of the present investigation is to study the effect of anisotropy of the underlying porous medium on the seepage characteristics, when the flow takes place under the structure. An investigation into the influence of anisotropy is of particular importance, in view of the fact that most soils display a directional variation with respect to permeability (Casagrande, 1940), which lends them the property of anisotropy. Significant anisotropic properties of soils have been reported by many investigators (Krizek and Anand, 1968). Not only naturally deposited soils but also soils deposited artificially for construction purposes exhibit stratification and hence anisotropy. From a mathematical point of view a vertical boundary-side in an anisotropic medium is transformed into an inclined one in a fictitious isotropic medium (Harr, 1962). As for the problem under investigation, the vertical sides of the depressed weir in the anisotropic medium can be taken to be inclined and embedded in a fictitious isotropic medium. The solution obtained in the transformed region can, of course, be interpreted in terms of the physical parameters in the original anisotropic region (Harr, 1962). It is with this conception that a solution has been attempted to a problem of flow around a depressed weir in an isotropic medium with inclined sides. The depth of the underlying medium is taken to be infinite. The angle of inclination of the sides has been made to lie in the range of  $0^\circ$  to  $180^\circ$ . The method of Schwartz-Christoffel transformation (Palubari-nova-Kochina, 1962) has been made use of in obtaining the solution, which is presented in terms of hypergeometric function and beta function. The numerical results bring out the influence of the angle of inclination of the sides of the depressed weir and the ratio of the width of the structure to depth of embedment on the exit gradient and the pressure distribution.

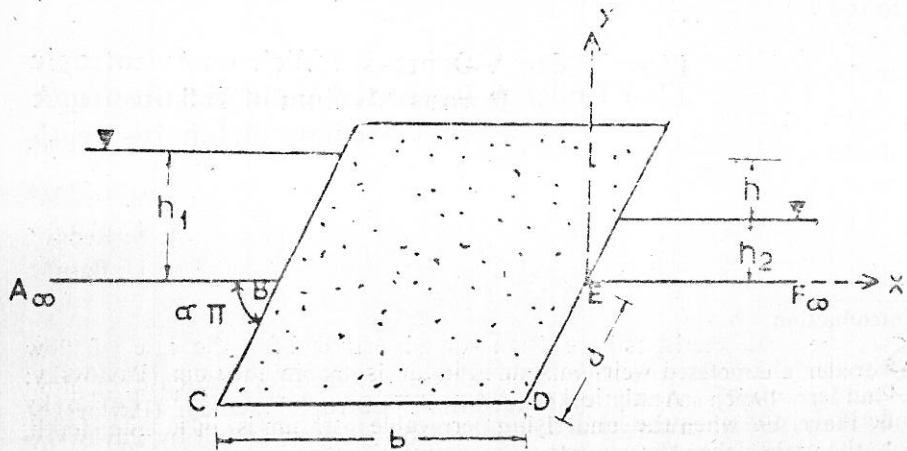
---

\* Professor, Department of Civil Engineering, Indian Institute of Science, Bangalore-12.

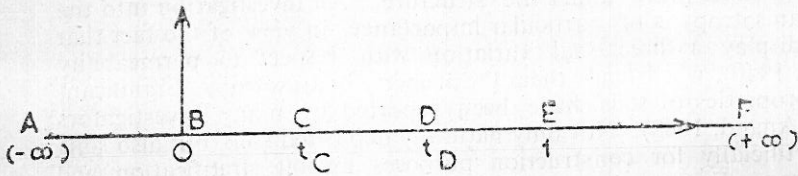
\*\* Senior Research Fellow, Department of Civil Engineering, Indian Institute of Science, Bangalore-12.

*The paper is open for discussion till the end of January 1976.*

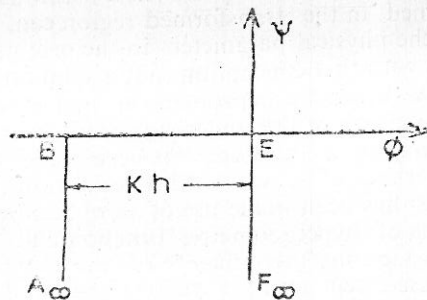
It is to be remembered, however, that the problem of flow around a depressed weir with vertical sides and that of the flow around an inclined sheet pile are but particular cases of the one presented herein.



(a) Z PLANE



(b) t PLANE



(c) W PLANE

FIGURE 1. Steps of conformal mapping.

**Analysis**

The transformation from the actual anisotropic  $z'$  ( $z' = x' + iy'$ ) plane to the fictitious isotropic  $z$  ( $z = x + iy$ ) plane is given by

$$x = x' (N^2 \sin^2 \theta + \cos^2 \theta)^{1/2} + y' \sin \theta \cos \theta (N^2 - 1) [N^2 \sin^2 \theta + \cos^2 \theta]^{-1/2};$$

and  $y = y' N (N^2 \sin^2 \theta + \cos^2 \theta)^{-1/2};$

where  $N = (k_\mu / k_\lambda)^{1/2}$ ;  $k_\mu$  and  $k_\lambda$  = the maximum and minimum coefficients of permeability, respectively; and  $\theta$  = angle made by the direction of maximum coefficient of permeability with the positive direction of  $x$ -axis, measured in the clockwise direction from  $x$ -axis.

If  $b'$  is the base width of the depressed weir in the actual physical plane, then the base width,  $b$ , in the fictitious plane is given by

$$b = b' (\cos^2 \theta + N^2 \sin^2 \theta)^{1/2}$$

Similarly, if  $d'$  is the depth of the vertical side in the actual physical plane, then the length,  $d$ , of the corresponding side which becomes inclined in the fictitious plane is given by

$$d = d' (\sin^2 \theta + N^2 \cos^2 \theta)^{1/2};$$

and, the angle of inclination,  $\alpha\pi$  [see Figure 1 a], is given by

$$\alpha\pi = \pi - \theta - \tan^{-1} [-\sqrt{N} \cot \theta]$$

where  $\theta\gamma = \tan^{-1} [\sqrt{N} \tan \theta]$

The coefficient of permeability  $k$ , in the fictitious isotropic plane is given by

$$k = (k_\mu \cdot k_\lambda)^{1/2}$$

The flow region in the fictitious isotropic  $z$ -plane is illustrated in Fig. 1(a). The region ABCDEFA is transformed on to the lower half of the auxiliary  $t$ -plane [Fig. 1(b)], using Schwartz-Christoffel transformation, the points,  $A, B, C, D, E$  and  $F$  being mapped onto  $-\infty, 0, t_C, t_D, l$  and  $\infty$  respectively. The  $z$ - $t$  relations corresponding to different ranges of values of  $t$  are as follows :

For  $0 \leq t \leq t_C$  :

$$\frac{dz}{dt} = \frac{M}{t^{1-\alpha} (t-t_C)^{\alpha-1} (t-t_D)^{-\alpha} (t-l)^\alpha} \quad \dots (1)$$

where,  $\alpha\pi$  = angle of inclination of side  $BC$  as shown in Fig. 1(a). From Equation (1), one gets

$$z = M \int_0^t t^{\alpha-1} (t-t_C)^{1-\alpha} (t-t_D)^\alpha (t-l)^{-\alpha} dt + z_B \quad \dots (2)$$

where  $z_B$  =  $z$ -coordinate of point  $B$  in the  $z$ -plane; and

$M$  = arbitrary constant.

Integration of Equation (2) gives rise to

$$z = (-1)^{1-\alpha} M t_C t_D^\alpha [B_r(\alpha, 2-\alpha) x F_1(\alpha, \alpha, -\alpha; 2; t_C, t_C/t_D) - r^\alpha (1-r)^{2-\alpha} \left\{ \frac{1}{\alpha} F_1(\alpha, \alpha, -\alpha; 2; t_C, t_C/t_D) {}_2F_1(2, 1; \alpha+1; r) \right\}]$$

$$- \sum_{n=0}^{n=\infty} R_n \frac{r^n}{\alpha+n} {}_2F_1(2+n, 1; \alpha+n+1; r) \Big\} + z_B \quad \dots (3)$$

where,

$$R_n = P_n Q_0 + P_{n-1} Q_1 + \dots + P_1 Q_{n-1} + P_0 Q_n; n = 0, 1, 2, \dots$$

$$P_n = \frac{\alpha(\alpha+1) \dots (\alpha+n-1)}{n!} t_C^{n-1}; n = 1, 2, \dots$$

$$Q_n = \frac{(-\alpha)(-\alpha+1) \dots (-\alpha+n-1)}{n!} \left(\frac{t_C}{t_D}\right)^n; n = 1, 2, \dots$$

$$r = \frac{t}{t_C}; P_0 = Q_0 = 1;$$

- $B_r(\quad)$  = incomplete beta function;
- $F_1(\quad)$  = hypergeometric function of two variables; and
- ${}_2F_1(\quad)$  = hypergeometric function of single variable.

with the condition  $z = z_C$ , when  $t = t_C$ , Equation (3) can be written as

$$|z_C - z_B| = |M| \cdot |(-1)^{1-\alpha} t_C t_D^\alpha B(\alpha, 2-\alpha) \times F_1(\alpha, \alpha, -\alpha; 2; t_C, t_C/t_D)| \quad \dots (4)$$

where,

$$B(\quad) = \text{complete beta function.}$$

For  $t_C \leq t \leq t_D$ :

The  $z-t$  relation is given by

$$z = M \int_{t_D}^t t^{\alpha-1} (t-t_C)^{1-\alpha} (t-t_D)^\alpha (t-1)^{-\alpha} dt + z_D \quad \dots (5)$$

where,

$z_D = z$ -coordinate of point  $D$  in the  $z$ -plane.

Integrating Equation (5) one obtains

$$z = M \cdot P \cdot \left[ B_r(\alpha+1, 2-\alpha) \times F_1(\alpha+1, 2, 1-\alpha; 3; \frac{t_D-t_C}{1-t_C}, \frac{t_D-t_C}{(1-t_C)t_D}) - r^{\alpha+1} (1-r)^{2-\alpha} \left\{ \frac{1}{\alpha+1} F_1(\alpha+1, 2, 1-\alpha; 3; \frac{t_D-t_C}{1-t_C}, \frac{t_D-t_C}{(1-t_C)t_D}) \times {}_2F_1(3, 1; \alpha+2; r) - \sum_{n=0}^{n=\infty} R'_n \frac{r^n}{\alpha+1+n} {}_2F_1(3+n, 1, \alpha+n+2, r) \right\} \right] + z_D \quad \dots (6)$$

where,  $R'_n = P'_n Q'_0 + P'_{n-1} Q'_1 + \dots + P'_1 Q'_{n-1} + P'_0 Q'_n; n = 0, 1, 2,$

$$\begin{aligned}
 P'_n &= \frac{2(2+1) \dots (2+n-1)}{n!} \left( \frac{t_D - t_C}{1 - t_C} \right)^n; n = 1, 2, \dots \\
 Q'_n &= \frac{(1-\alpha)(1-\alpha+1) \dots (1-\alpha+n-1)}{n!} \left[ \frac{(t_D - t_C)}{(1-t_C)t_D} \right]^n; n=1,2,\dots \\
 P'_o &= Q'_o = 1; \\
 P &= \frac{(t_D - t_C)^2 (1-t_D)}{t_D^{1-\alpha} (1-t_C)^{1+\alpha}}; \text{ and} \\
 r &= (1-t_C)(t_D-t)/(t_D-t_C)(1-t).
 \end{aligned}$$

with the condition  $z = z_C$ , when  $t = t_C$ , Equation (6) can be written as  $|z_C - z_D| = |M| \cdot |P \cdot B(\alpha+1, 2-\alpha) \times$

$$F_1(\alpha+1, 2, 1-\alpha; 3; \frac{t_D - t_C}{1 - t_C}, \frac{t_D - t_C}{(1-t_C)t_D}) \Big| \dots (7)$$

For  $t_D \leq t \leq 1$ :

The  $z-t$  relation is given by

$$z = M \int_{t_E}^t t^{\alpha-1} (t-t_C)^{1-\alpha} (t-t_D)^\alpha (t-1)^{-\alpha} dt + z_E \dots (8)$$

where,  $z_E = z$ -coordinate of point  $E$  in  $z$ -plane.

Integration of Equation (8) leads to

$$\begin{aligned}
 z &= (-1)^{-\alpha} M (1-t_D) (1-t_C)^{1-\alpha} [B_r(1-\alpha, 1+\alpha) \times \\
 &F_1(1-\alpha, 1-\alpha, \alpha-1; 2; 1-t_D, \frac{1-t_D}{1-t_C}) \\
 &- r^{1-\alpha} (1-r)^{1+\alpha} \left\{ \frac{1}{1-\alpha} \cdot F_1(1-\alpha, 1-\alpha, \alpha-1; 2; 1-t_D, \frac{1-t_D}{1-t_C}) \right. \\
 &\times {}_2F_1(2, 1; 2-\alpha; r) \\
 &\left. - \sum_{n=0}^{n=\infty} R_n^n \frac{r^n}{1-\alpha+n} {}_2F_1(2+n, 1; 2-\alpha+n; r) \right\}] + z_E \dots (9)
 \end{aligned}$$

where,

$$\begin{aligned}
 R_n^n &= P_n^n Q_o^n + P_{n-1}^n Q_1^n + \dots + P_1^n Q_{n-1}^n + P_o^n Q_n^n; n = 0, 1, 2, \dots \\
 P_n^n &= \frac{(1-\alpha)(1-\alpha+1) \dots (1-\alpha+n-1)}{n!} (1-t_D)^n; n = 1, 2, \dots \\
 Q_n^n &= \frac{(\alpha-1)(\alpha)(\alpha+1) \dots (\alpha-1+n-1)}{n!} \left( \frac{1-t_D}{1-t_C} \right)^n; n = 1, 2, \dots \\
 r &= \frac{(t-1)}{(t_D-1)}; \text{ and } P_o^n = Q_o^n = 1.
 \end{aligned}$$

With the condition  $z = z_D$ , when  $t = t_D$ , Equation (9) can be written as  $|z_D - z_E| = |M| \cdot |(-1)^{-\alpha}(1-t_D) (1-t_C)^{1-\alpha} B(1-\alpha, 1+\alpha) \times$

$$F_1(1-\alpha, 1-\alpha, \alpha-1; 2; 1-t_D, \frac{1-t_D}{1-t_C}) \Big| \dots (10)$$

The three unknown quantities  $M$ ,  $t_C$  and  $t_D$  can be obtained by solving the three Equations (4), (7) and (10). Hence the correspondence between the  $z$  and  $t$ -planes is complete.

### Exit Gradient Distribution

For the range  $EF$  in the  $z$ -plane, the correspondence with the  $t$ -plane is obtained (for  $1 \leq t \leq \infty$ ) as

$$z = M \int_{t_E}^t t^{\alpha-1} (t-t_C)^{1-\alpha} (t-t_D)^\alpha (t-1)^{-\alpha} dt + z_E \quad \dots (11)$$

On integration, Equation (11) reduces to

$$\begin{aligned} |z - z_E| = |M| \cdot \left[ -\frac{A_0 (1-r)^{1-\alpha}}{r} + (A_0 \alpha - A_1) I_1 \right. \\ \left. + \sum_{n=2}^{n-\infty} A_n \left\{ \frac{B_1}{t} (n-1, 1-\alpha) - B (n-1, 1-\alpha) \right\} \right] \quad \dots (12) \end{aligned}$$

where,

$$A_n = (C_n D_0 + C_{n-1} D_1 + \dots + C_0 D_n); n = 0, 1, 2, \dots$$

$$C_n = \frac{(-1)^n (1-\alpha) (1-\alpha-1) \dots (1-\alpha-n-1) t^n}{n!}; n = 1, 2, \dots$$

$$D_n = \frac{(-1)^n \alpha (\alpha-1) (\alpha-2) \dots (\alpha-n-1) t^n}{n!}; n = 1, 2, \dots$$

$$C_0 = D_0 = 1;$$

$$r = \frac{1}{t}; \text{ and}$$

$$I_1 = \int_r^1 \frac{(1-r)^{-\alpha}}{r} dr$$

### Expression for Exit Gradient

Exit gradient  $I_E$  is given by

$$I_E = \frac{i}{k} \frac{dw/dz}{dt/dt} \quad \dots (13)$$

where,

$k$  = coefficient of permeability. In order to arrive at an expression for  $I_E$ , the quantity  $dw/dt$  needs to be known. An expression for  $dw/dt$  is developed in the following manner:

$w-t$  relation:

The function  $w$  is defined as

$$w = \phi + i\psi \quad \dots (14)$$

where,

$\phi$  = velocity potential, and  
 $\psi$  = stream function.

The  $w$ -plane, illustrated in Figure 1(c) is transformed onto the lower half of the auxiliary  $t$ -plane.

Applying Schwartz-Christoffel transformation to the region in the  $w$ -plane, one gets the  $w$ - $t$  relation as

$$dw = \frac{-\sqrt{-1} kh}{\pi \sqrt{t(t-1)}} dt \quad \dots (15)$$

where  $h$  = head difference between upstream and downstream water levels, as in Figure 1 (a).

Hence,  $I_E$  is given by

$$I_E = \frac{i}{k} \frac{dw}{dt} \bigg| \frac{dz}{dt}$$

$$= \frac{h}{\pi} \cdot \frac{1}{\sqrt{t(t-1)}} \cdot \frac{1}{M t^{\alpha-1} (t-t_C)^{1-\alpha} (t-t_D)^{\alpha} (t-1)^{-\alpha}} \quad \dots (16)$$

**Pressure Distribution**

From Equation (15), one obtains the expression for  $w$  as

$$w = \frac{-2 kh}{\pi} \cos^{-1} \sqrt{t} \quad \dots (17)$$

Now, since  $w = \phi + i\psi$ , and  $\psi = 0$  along  $BC, CD$  and  $DE$ , one can write

$$\phi = \frac{-2 kh}{\pi} \cos^{-1} \sqrt{t} \quad \dots (18)$$

But,

$$\phi = -k \left( \frac{p}{\gamma_w} + y \right) + C \quad \dots (19)$$

where,

- $p$  = pressure at a point;
  - $\gamma_w$  = unit weight of water;
  - $y$  = elevation head at a point;
- and  $C$  = constant =  $k(h_1 - h)$ , with  $h_1$ , as upstream head.

The uplift pressure along the base  $CD$  of the depressed structure can, therefore, be obtained from Equations (18) and (19) as

$$p = \gamma_w \left[ \frac{2h \cos^{-1} \sqrt{t}}{\pi} + h_1 - h + y \right] \quad \dots (20)$$

where  $t_C \leq t \leq t_D$

**Results and discussion**

Numerical results have been presented for the cases of

- (i)  $\alpha < \frac{1}{2}$ ;
- and (ii)  $\alpha > \frac{1}{2}$ .

In case (i), the values of  $\alpha$  have been taken to be  $\frac{1}{6}$ ,  $\frac{1}{4}$ ,  $\frac{1}{3}$  and  $\frac{5}{12}$ , and in case (ii), the values of  $\alpha$  have been taken to be  $\frac{7}{12}$ ,  $\frac{2}{3}$  and  $\frac{3}{4}$ .

In each of the cases the ratio of the width of the structure to the depth of embedment has been varied keeping the value of  $\alpha$  constant.

In doing the computations, care has been taken to see that the summation of an infinite series is done to get a 6 digit accuracy.

In presenting the results in graphical form, the width of the structure,  $|z_D - z_C|$  has been denoted as  $b$ , and the length along the inclined sides (either  $|z_D - z_E|$  or  $|z_C - z_B|$ ) has been denoted by  $d$ . Since  $z_E = 0$ ,  $|z - z_E|$  along the downstream side  $EF$  (Figure 1 a) is denoted by  $z$ , in presenting the exit gradient distribution.

Figure 2 to Figure 5 show the variation of exit gradient presented in nondimensional form as  $I_E \frac{d}{h}$ , with the nondimensional parameter  $\frac{b}{d}$ , for  $\alpha = \frac{1}{6}$ ,  $\frac{1}{4}$ ,  $\frac{1}{3}$  and  $\frac{5}{12}$ . Figure 6 to Figure 8 show the same for values of  $\alpha = \frac{7}{12}$ ,  $\frac{2}{3}$  and  $\frac{3}{4}$ .

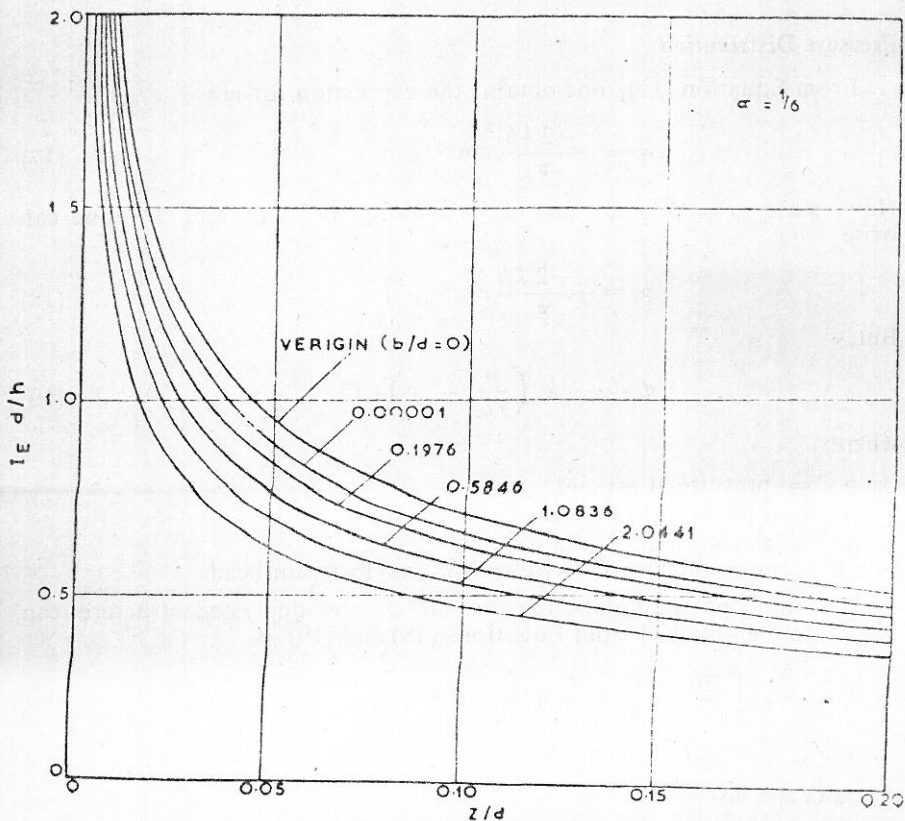


FIGURE 2. Exit gradient distribution for  $\alpha = 1/6$



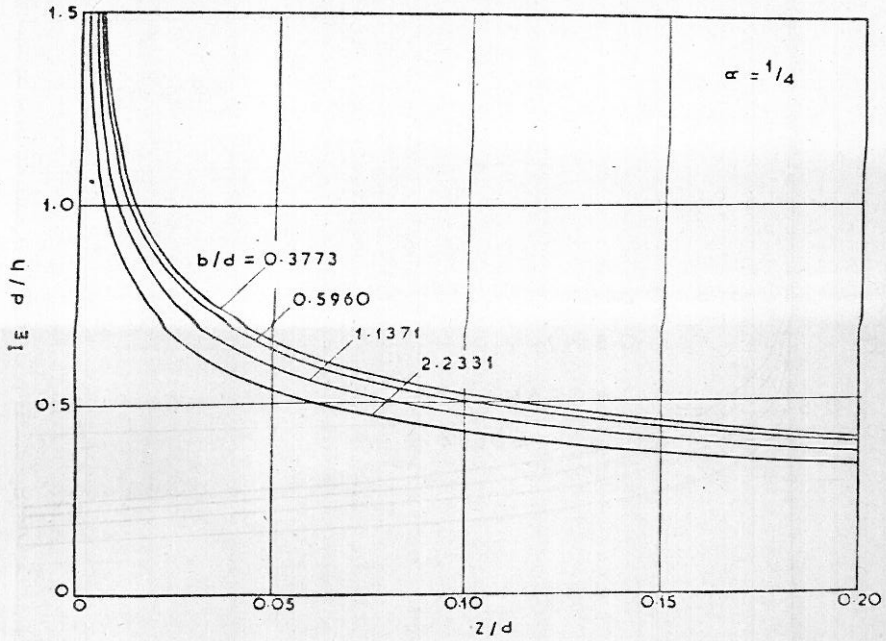


FIGURE 3. Exit gradient distribution for  $\alpha = 1/4$

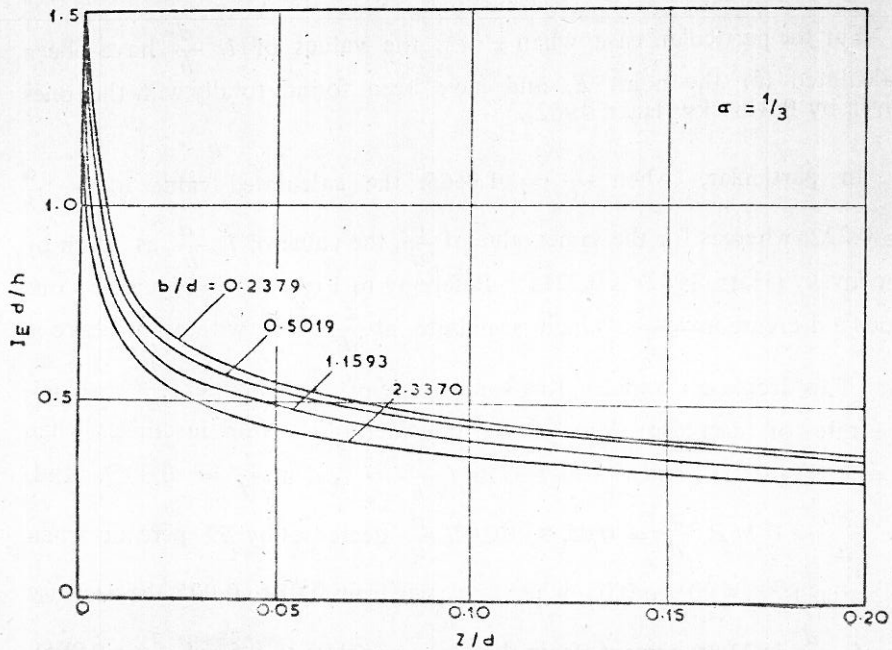


FIGURE 4. Exit gradient distribution for  $\alpha = 1/3$

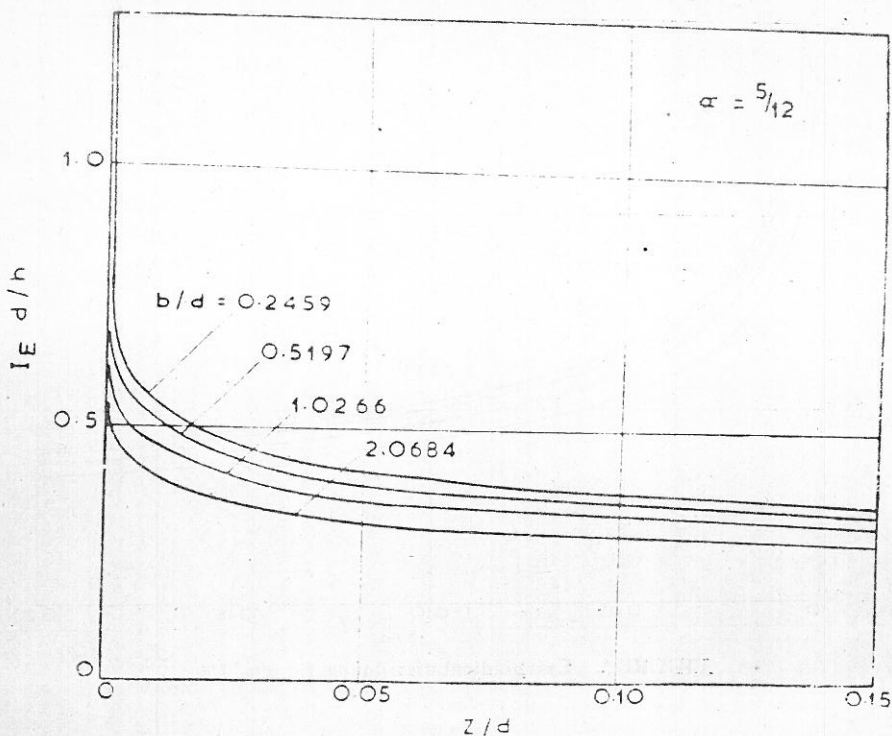


FIGURE 5. Exit gradient distribution for  $\alpha = 5/12$

For the particular case when  $\alpha = \frac{1}{2}$ , the values of  $I_E \frac{d}{h}$  have been calculated for the point  $E$ , and have been found totally with the ones given by Pavlovsky (Harr, 1962).

In particular, when  $\frac{b}{d} = 1.0665$ , the calculated value of  $I_E \frac{d}{h} = 0.222$ , whereas for the same value of  $\frac{b}{d}$ , the value of  $I_E \frac{d}{h}$  as given by Pavlovsky (Harr, 1962) is 0.2215. Referring to Figure 2 to Figure 5, one finds a decrease in  $I_E \frac{d}{h}$  (which is infinite at  $\frac{z}{d} = 0$ ), with an increase in  $\frac{z}{d}$ . This decrease is rapid upto a small value of  $\frac{z}{d}$ ; at larger  $\frac{z}{d}$  values, the rate of decrease slows down considerably. For instance, when  $\alpha = \frac{1}{6}$  (Figure 2), and  $\frac{b}{d} = 1.0836$ ,  $I_E \frac{d}{h} = 1.71$  at  $\frac{z}{d} = 0.005$ , and,  $I_E \frac{d}{h} = 0.7$  at  $\frac{z}{d} = 0.05$ , so that  $I_E \frac{d}{h}$  decreases by 59 percent when  $\frac{z}{d}$  varies from 0.005 to 0.05, when  $\frac{z}{d}$  varies from 0.05 to 0.095, the decrease in  $I_E \frac{d}{h}$  is 22.85 percent (from 0.7 at  $\frac{z}{d} = 0.05$  to 0.54 at  $\frac{z}{d} = 0.095$ ).

For  $\frac{z}{d} > 0.20$ , there is no appreciable change in  $I_E \frac{d}{h}$ , with increase in  $\frac{z}{d}$ .

At a constant value of  $\alpha$  ( $\alpha < \frac{1}{2}$ ), an increase in  $\frac{b}{d}$  ratio effects a decrease in  $I_E \frac{d}{h}$  at a given  $\frac{z}{d}$  (Figures 2 to 5).

An increase in  $\alpha$  bring in a noticeable change in the exit gradient distribution (Figures 2 to 5). The value of  $\frac{z}{d}$  from which a further increase would have negligible effect on the rate of decrease of  $I_E \frac{d}{h}$ , would recede more towards 0, as  $\alpha$  increases. This is true for all  $\frac{b}{d}$  ratios.

For  $\alpha > \frac{1}{2}$ ,  $I_E \frac{d}{h}$  starts from 0 at  $\frac{z}{d} = 0$ , reaches a maximum and then decreases monotonically as  $\frac{z}{d}$  increases (Figures 6 to 8). The maximum  $I_E \frac{d}{h}$  at a constant  $\alpha$  decreases as  $\frac{b}{d}$  increases, and also occurs at larger  $\frac{z}{d}$  values. In particular, when  $\alpha = \frac{7}{12}$  (Figure 6), and  $\frac{b}{d} = 0.2402$ , maxi-

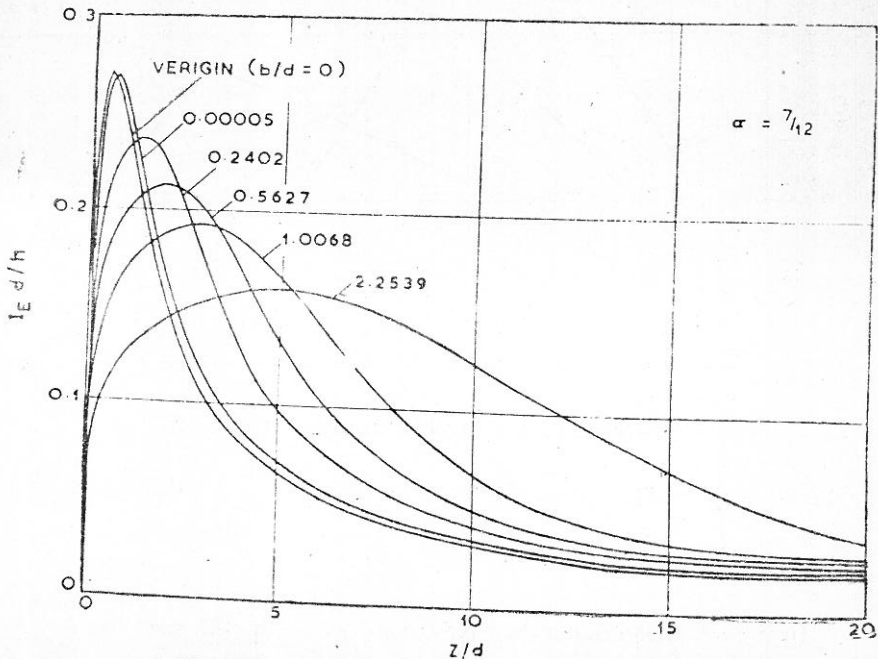


FIGURE 6. Exit gradient distribution for  $\alpha = \frac{7}{12}$

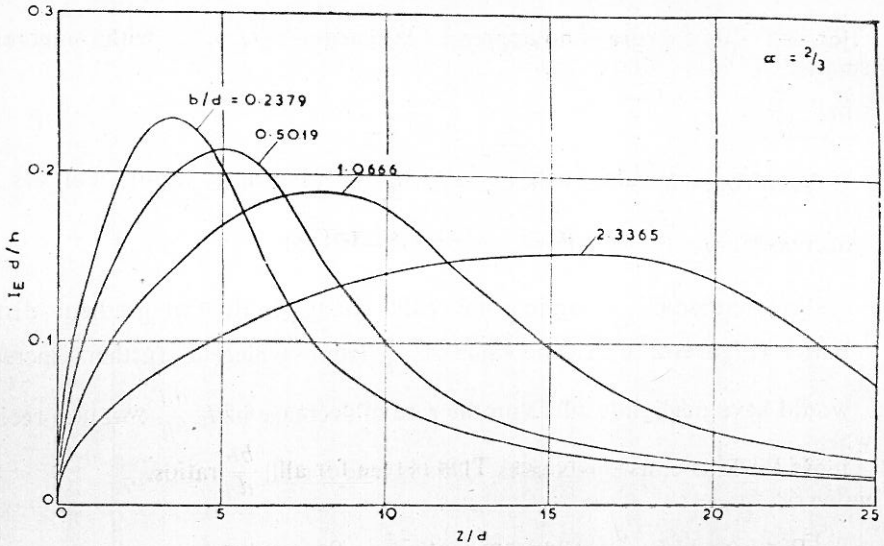


FIGURE 7. Exit gradient distribution for  $\alpha = 2/3$

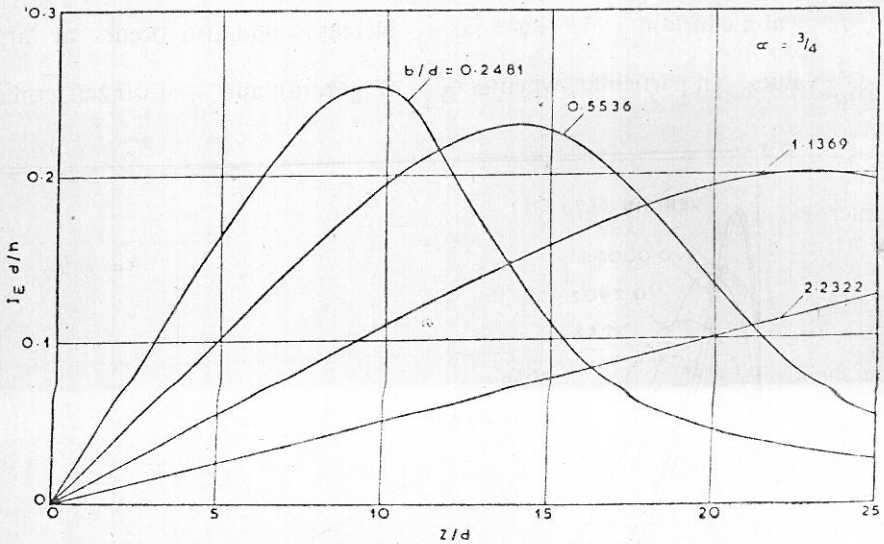


FIGURE 8. Exit gradient distribution for  $\alpha = 3/4$

imum  $I_E \frac{d}{h}$  is 0.236 at  $\frac{z}{d} = 1.4$ ; whereas, for  $\frac{b}{d} = 0.5627$ , maximum  $I_E \frac{d}{h}$  is 0.213 at  $\frac{z}{d} = 1.9$ .

In Figures 2 and 6, curves have been drawn for the case of  $\frac{b}{d} = 0$ , which corresponds to the case of flow around an inclined sheet pile for

which solution was given by Verigin (vide Harr, 1962). As  $\frac{b}{d}$  becomes smaller, the curves approach the one given by Verigin. Curves for very small values of  $\frac{b}{d} = 0.00001$  and  $\frac{b}{d} = 0.00005$  have been plotted in Figures 2 and 6, for  $\alpha = \frac{1}{6}$  and  $\alpha = \frac{7}{12}$  respectively, to illustrate this point.

The influence of  $\frac{b}{d}$  on  $-\frac{\phi_D}{kh}$  ( $= -\frac{\phi}{kh}$  at the point  $D$  in Figure 1 (a)) for various values of  $\alpha$  has been illustrated in Figure 9. An increase in  $\frac{b}{d}$  is seen to effect a decrease in  $-\frac{\phi_D}{kh}$ , at a constant  $\alpha$ . In particular, when  $\alpha = \frac{1}{6}$ , and  $\frac{b}{d} = 0.2$ ,  $-\frac{\phi_D}{kh} = 0.595$ ; whereas, for the same value of  $\alpha$ , and  $\frac{b}{d} = 3.0$ ,  $-\frac{\phi_D}{kh} = 0.29$ ; which shows that, a decrease of 51.26 percent in  $-\frac{\phi_D}{kh}$  occurs when  $\frac{b}{d}$  increases from 0.2 to 3.0. The decrease in  $-\frac{\phi_D}{kh}$  is 24.13 percent as  $\frac{b}{d}$  increases from 3.0 (when  $-\frac{\phi_D}{kh} = 0.29$ ) to 5.8 (when  $-\frac{\phi_D}{kh} = 0.22$ ). Thus, the rate of decrease of  $-\frac{\phi_D}{kh}$  is rapid within a small range of  $\frac{b}{d}$ , and slower at larger values of  $\frac{b}{d}$ . For  $\frac{b}{d} > 10$ , there is no appreciable change in  $-\frac{\phi_D}{kh}$ , for an increase in  $\frac{b}{d}$ .

For  $\frac{b}{d} = 0$ , the value of  $-\frac{\phi_D}{kh}$  corresponds to the value at the tip of a sheet pile. For  $\alpha = \frac{1}{6}$ ,  $-\frac{\phi_D}{kh}$ , using Verigin's solution, is 0.732. In the present approach, when  $\alpha = \frac{1}{6}$ , and  $\frac{b}{d} = 0.2$ ,  $-\frac{\phi_D}{kh} = 0.595$ ; also, when  $\alpha = \frac{1}{6}$  and  $\frac{b}{d} = 0.00005$ ,  $-\frac{\phi_D}{kh} = 0.729$ , approaching the one obtained using Verigin's solution, as  $\frac{b}{d} \rightarrow 0$ . The influence of  $\frac{b}{d}$  on  $-\frac{\phi_C}{kh}$  ( $= -\frac{\phi}{kh}$  at the point  $C$  in Figure 1 (a)) has been shown in Figure 10. At constant  $\alpha$ , as  $\frac{b}{d}$  increases from 0,  $-\frac{\phi_C}{kh}$  increases rapidly over a small range of value of  $\frac{b}{d}$  and for larger value of  $\frac{b}{d}$ , the rate of increase of  $-\frac{\phi_C}{kh}$  is slow.

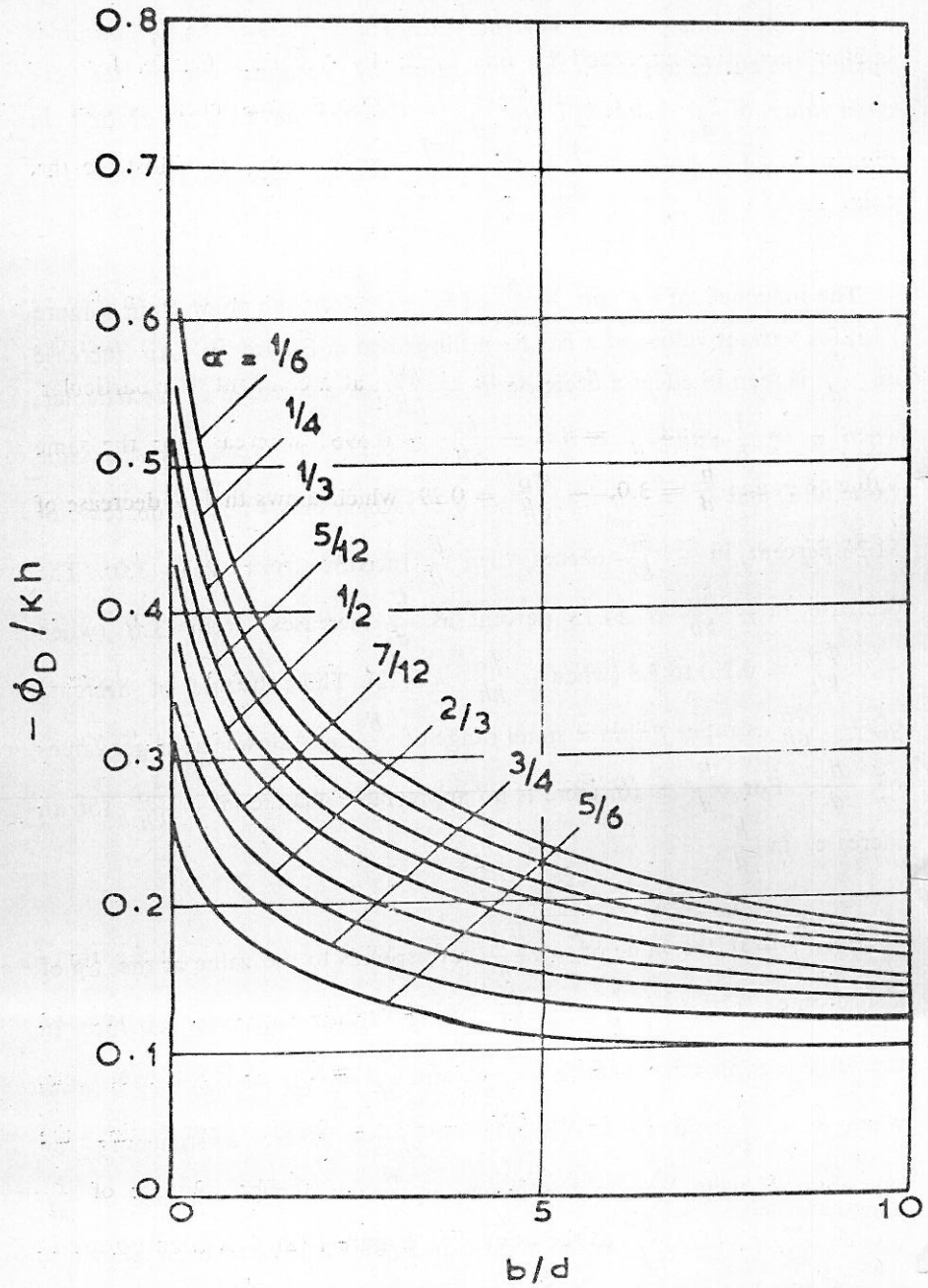


FIGURE 9, Variation of  $\frac{\phi_D}{kh}$  with  $\frac{b}{d}$  for various  $\alpha$

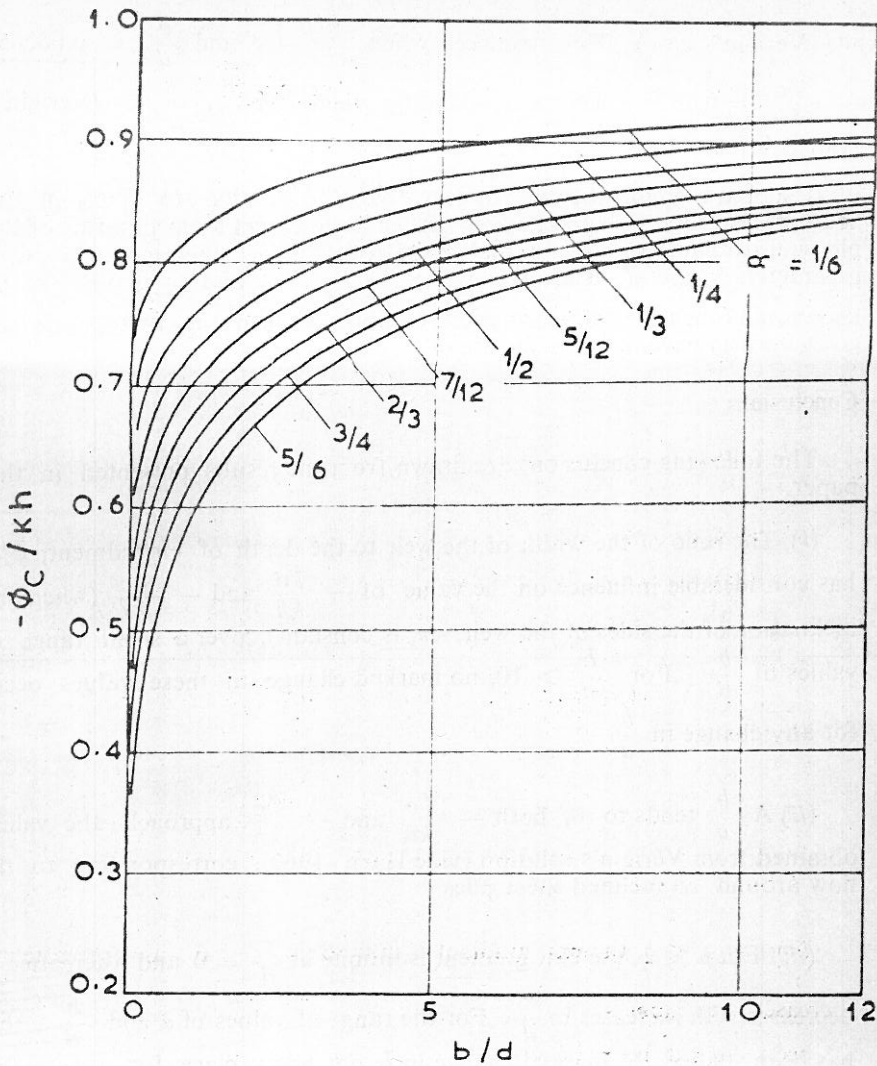


FIGURE 10. Variation of  $\frac{\phi_c}{kh}$  with  $\frac{b}{d}$  for various  $\alpha$ .

For example, when  $\alpha = \frac{5}{6}$ ,  $-\frac{\phi_c}{kh}$  increases by 96.8 percent as  $\frac{b}{d}$  increases from 0.1 to 5; whereas, the increase in  $-\frac{\phi_c}{kh}$  is by 10.3 percent as  $\frac{b}{d}$  increases from 5 to 9.9. For  $\frac{b}{d} > 10$ , no appreciable change in  $-\frac{\phi_c}{kh}$  occurs for an increase in  $\frac{b}{d}$ . As  $\frac{b}{d} \rightarrow 0$  at a constant  $\alpha$ , the value of  $-\frac{\phi_c}{kh}$  approaches the one corresponding to the tip of a sheet

pile (Verigin's case). For instance, when  $\alpha = \frac{1}{6}$ , and  $\frac{b}{d} = 0.00005$ ,  $-\frac{\phi_c}{kh} = 0.7325$ . The corresponding value for  $\frac{b}{d} = 0$  (Verigin's case) is 0.732.

It should be remembered, however, that the results are given in the fictitious isotropic plane, and in order to interpret them in terms of the physical parameters in the actual anisotropic plane, the actual physical parameters  $b'$  and  $d'$ , as also the values of  $k_\mu$ ,  $k_\lambda$  and  $\theta$  have to be known, and then the transformation relations between the two planes (as given earlier) have to be made use of.

### Conclusions

The following conclusions are drawn from the results presented in this paper.

(i) The ratio of the width of the weir to the depth of embedment,  $b/d$ , has considerable influence on the value of  $-\frac{\phi_D}{kh}$  and  $-\frac{\phi_c}{kh}$  (when the inclination of the sides of the weir,  $\alpha\pi$ , is constant), over a small range of values of  $\frac{b}{d}$ . For  $\frac{b}{d} > 10$ , no marked change in these values occur for any change in  $\frac{b}{d}$ .

(ii) As  $\frac{b}{d}$  tends to 0, both  $-\frac{\phi_D}{kh}$  and  $-\frac{\phi_c}{kh}$  approach the values obtained from Verigin's solution (vide Harr, 1962), corresponding to the flow around an inclined sheet pile.

(iii) For  $\alpha < \frac{1}{2}$ , the exit gradient is infinite at  $\frac{z}{d} = 0$  and thereafter it decreases with increases in  $\frac{z}{d}$ . For the range of values of  $\alpha$  and  $\frac{b}{d}$  that has been studied, no marked change in  $I_E d/h$  takes place for  $z/d > 0.2$ . It can be concluded, however, that this trend will be true for larger  $\frac{b}{d}$  ratios as well.

(iv) For  $\alpha > \frac{1}{2}$ ,  $I_E d/h$  starts from 0 at  $\frac{z}{d} = 0$ , increases to a maximum value and then decreases monotonically as  $\frac{z}{d}$  increases. The maximum  $I_E d/h$  decreases as  $\frac{b}{d}$  ratio increases at constant  $\alpha$ .

(v) As  $b/d$  tends to 0, the exit gradient distribution at a constant  $\alpha$  approaches the one obtained from Verigin's solution. This would be true for all values of  $\alpha$  lying between  $0^\circ$  and  $180^\circ$ .



(vi) For  $\alpha = \frac{1}{2}$ , the results correspond to those given by Pavlovsky (Vide Harr, 1962), for flow under a weir on isotropic medium of infinite depth.

(vii) The inclination of the sides of the weir,  $\alpha\pi$ , has considerable influence on the values of  $-\frac{\phi_D}{kh}$  and  $-\frac{\phi_C}{kh}$ . At constant  $\frac{b}{d}$  ratio, both  $-\frac{\phi_D}{kh}$  and  $-\frac{\phi_C}{kh}$  decrease as  $\alpha$  increases.

(viii) Knowing the nature of anisotropy, represented by the value of  $k_\mu$ ,  $k_\lambda$  and  $\theta$ , the pressure distribution and the exit gradient for any particular physical problem can be obtained by using the analysis presented.

### References

- BATEMAN, H. (1953) : "Higher Transcendental Functions". Vol. 1, McGraw-Hill Book Company, Inc., New York.
- BURINGTON, R.S. (1940) : "Handbook of Mathematical Tables and Formulas". 3rd ed., Handbook Publishers, Inc., Sandusky, Ohio.
- CASAGRANDE, A. (1940) : "Seepage through Dams". *Contributions to Soil Mechanics 1925-1940*, Boston Society of Civil Engineers, Boston.
- HARR, M.E. (1962) : "Groundwater and Seepage". McGraw Hill Book Company, Inc., New York.
- KRIZEK, R.J. and ANAND, V.B. (1968) : "Flow Around a Vertical Sheet Pile Embedded in an Inclined Stratified Medium". *Water Resources Research*. Vol. 4, No. 1, February, pp. 113-123.
- PALUBARINOVA-KOCHINA, P. YA. (1962) : "Theory of Groundwater Movement". Translated from the Russian by J.M. Roger De Wiest, Princeton University Press, Princeton, New Jersey.